

# The Cosmic Crystallinity Conundrum: Clues from IRAS 17495–2534

Angela K. Speck<sup>1,2</sup>, Alan G. Whittington<sup>2</sup> Josh B. Tartar<sup>1</sup>

## ABSTRACT

Since their discovery, cosmic crystalline silicates have presented several challenges to understanding dust formation and evolution. The mid-infrared spectrum of IRAS 17495–2534, a highly obscured oxygen-rich asymptotic giant branch (AGB) star, is the only source observed to date which exhibits a clear crystalline silicate absorption feature. This provides an unprecedented opportunity to test competing hypotheses for dust formation. Observed spectral features suggest that both amorphous and crystalline dust is dominated by forsterite ( $\text{Mg}_2\text{SiO}_4$ ) rather than enstatite ( $\text{MgSiO}_3$ ) or other silicate compositions. We confirm that high mass-loss rates should produce more crystalline material, and show why this should be dominated by forsterite. The presence of  $\text{Mg}_2\text{SiO}_4$  glass suggests that another factor (possibly C/O) is critical in determining astromineralogy. Correlation between crystallinity, mass-loss rate and initial stellar mass suggests that only the most massive AGB stars contribute significant quantities of crystalline material to the interstellar medium, resolving the conundrum of its low crystallinity.

*Subject headings:* stars: AGB and post-AGB — stars: individual (IRAS 17495-2534) — (stars:) circumstellar matter — (ISM:) dust, extinction — infrared: stars

## 1. Introduction

One of the most exciting recent developments in astronomy was the discovery of crystalline silicate stardust by the Infrared Space Observatory (ISO; de Graauw et al. 1996).

---

<sup>1</sup>Department of Physics and Astronomy, University of Missouri, Columbia, MO 65211

<sup>2</sup>Department of Geological Sciences, University of Missouri, Columbia, MO 65211

Crystalline silicates were initially discovered around evolved intermediate mass stars at far-infrared (IR) wavelengths (Waters et al. 1996), but have since been detected in young stellar objects (Waelkens et al. 1996), comets (Crovisier et al. 1996), and Ultra Luminous Infrared Galaxies (Spoon et al. 2006). In the interstellar medium (ISM) silicate grains in crystalline form are rare ( $\sim 1\%$  crystalline by mass; Min et al. 2007; Kemper et al. 2004). However, Asymptotic Giant Branch (AGB) stars and their successors (pre-planetary and planetary nebulae) are the major contributors of material to the ISM (Kwok 2004). It has been suggested that AGB stars could contain  $\gtrsim 10\%$  crystalline silicates (Kemper et al. 2004), so it is vital to understand the formation of dust around AGB stars to resolve this apparent discrepancy.

AGB stars are luminous cool giants, with high mass-loss rates ( $10^{-7} < \dot{M} < 10^{-3} M_{\odot}/\text{yr}$ ), which increase over time (van Loon et al. 2005). They are highly evolved descendants of low-to intermediate-mass ( $0.8\text{--}8 M_{\odot}$ ) stars. Mass loss produces a circumstellar envelope, where dust forms. The order in which different species condense from the outflowing gas depends on the physical conditions within the envelope. Once  $\dot{M}$  is very high the circumstellar shell becomes optically thick, even at IR wavelengths, and the silicate emission features absorb themselves. The dust mineralogy is dictated by the dust condensation sequence and depends strongly on  $\dot{M}$  (Dijkstra et al. 2005). Blommaert et al. (2007) showed that the mineralogy depends only on the age of the star for a given initial stellar mass.

To date, crystalline silicate features have been seen clearly only in emission. It has been proposed that crystalline silicate absorption at  $11\mu\text{m}$  contributes to the broadening of the classic  $10\mu\text{m}$  amorphous silicate absorption feature associated with OH/IR stars (Sylvester et al. 1999; Vanhollebeke 2007). However, IRAS 17495–2534 (hereafter I17495) is the first object to show a distinct crystalline  $11\mu\text{m}$  absorption feature.

I17495 is located in the Galactic Plane (gal. coord. = 003.6844+00.3880) at a distance of  $\sim 4\text{kpc}$  (Loup et al. 1993), about half way to the Galactic Center. The IRAS LRS spectrum clearly exhibits an  $11.1\mu\text{m}$  absorption feature superposed on the classic  $10\mu\text{m}$  amorphous silicate feature (Fig. 1). This is the first clear crystalline silicate absorption feature seen to date in any object.

$\dot{M}$  for this object is estimated to be  $\sim 2 \times 10^{-4} < \dot{M} < 5 \times 10^{-4} M_{\odot}/\text{yr}$  based on mid-IR ([25]-[12]) color (Loup et al. 1993) and the range of optical depths ( $15 < \tau_{10\mu\text{m}} < 45$ ) consistent with our model results (see § 3). Both  $\dot{M}$  and expansion velocity ( $v_{\text{exp}}$ ,  $16\text{km/s}$ ; Loup et al. 1993) are at the high end of normal for AGB stars. Most extreme O-rich AGB stars are OH/IR stars, exhibiting OH-maser emission. I17495 is one of a handful of visibly obscured O-rich AGB stars not exhibiting OH-maser emission (dubbed color-mimics; Lewis 1994). However, the spectra of other color mimics more closely resemble those of OH/IR

stars, i.e., when observed, the putative  $11\mu\text{m}$  crystalline silicate feature is merely a hump superposed on the regular amorphous silicate absorption feature. This is also true for OH/IR stars with similar mass-loss rates in the Galactic Bulge (GB). Even the GB source with the highest  $\dot{M}$  ( $3 \times 10^{-4} M_{\odot}/\text{yr}$ ; IRAS 17276–2846; Vanhollebeke 2007) shows the  $11\mu\text{m}$  feature as a hump, rather than the distinct  $11\mu\text{m}$  feature seen in Fig. 1.

While forsterite (crystalline  $\text{Mg}_2\text{SiO}_4$ ) is expected to have a peak near  $11.3\mu\text{m}$  (e.g. Koike et al. 2003), the peak can shift to shorter wavelengths. In the laboratory, Jäger et al. (1998) found that synthetic forsterite peaks closer to  $11.2\mu\text{m}$ , and matches the position of the hump observed in GB OH/IR stars (Vanhollebeke 2007). Fabian et al. (2001) investigated grain shape effects. Their mass absorption coefficients for ellipsoidal forsterite grains are included in Fig. 1, and demonstrate that the crystalline forsterite feature can peak at  $11.1\mu\text{m}$ . Boersma et al. (2008) attributed an  $11.1\mu\text{m}$  emission feature in the spectrum of a Herbig Ae/Be star to forsterite. Tamanai et al. (2006) found that, for non-embedded free-flying particles of forsterite, the feature actually peaks at  $11.06\mu\text{m}$ . Composition, grain-shape and grain-size can significantly shift the position of this feature.

## 2. Crystallinity & Mass-loss rates

Crystalline silicates were first observed around evolved stars with very high  $\dot{M}$ , leading to the inference that crystal formation requires such conditions (e.g. Cami et al. 1998). However, the diagnostic infrared features of crystalline grains can remain hidden by the strong amorphous silicate features until  $\dot{M} \approx 10^{-5} M_{\odot}/\text{yr}$  (Kemper et al. 2001).

Dust condensation temperature ( $T_{\text{dust}}$ ) are depressed at low gas pressures (Lodders & Fegley 1999; Gail & Sedlmayr 1999). Fig. 2 shows the calculated pressure-temperature (P–T) conditions in the dust-forming zone around O-rich AGB stars (see Dijkstra et al. 2005, for method), compared to thermodynamic equilibrium dust condensation models (Lodders & Fegley 1999), and the glass-transition temperatures ( $T_g$ ) for  $\text{Mg}_2\text{SiO}_4$  (Richet et al. 1993) and  $\text{MgSiO}_3$  (Wilding et al. 2004). Grains forming below  $T_g$  will be amorphous, while grains forming much above this temperature should crystallize rapidly (Sogawa & Kozasa 1999). For  $\dot{M} \lesssim 2 \times 10^{-7} M_{\odot}/\text{yr}$ ,  $T_{\text{dust}}$  for both  $\text{Mg}_2\text{SiO}_4$  and  $\text{MgSiO}_3$  fall below their respective  $T_g$ , thus precluding crystal formation. Above this threshold  $\dot{M}$ , dust grains should form at temperatures where crystalline structures would form either directly, or by annealing of initially amorphous grains. Once dust forms, the radial temperature profile steepens, because of absorption of starlight by dust grains. Including this factor, we can use the outflow velocity to calculate the timescale for dust to cool from  $T_{\text{dust}}$  to  $T_g$ . For  $\dot{M} > 10^{-5} M_{\odot}/\text{yr}$ , the timescale is  $\sim 6$ – $12$  months, providing ample time for annealing and crystallization. This

suggests that crystalline silicates should be more common in high  $\dot{M}$  stars and the observed  $\dot{M}$ –crystallinity correlation is not merely due to masking of the crystalline spectral features (c.f. Sogawa & Kozasa 1999). In addition, for stars with  $\dot{M} \gtrsim 10^{-5} M_{\odot}/\text{yr}$  forsterite forms at a higher temperature than enstatite (crystalline  $\text{MgSiO}_3$ ), and the difference in  $T_{\text{dust}}$  for these two species increases with  $\dot{M}$  (see § 4).

### 3. Radiative transfer (RT) modeling

We used the 1-D radiative transfer (RT) program DUSTY (Ivezic & Elitzur 1995), to determine the gross mineralogy associated with the mid-IR absorption features. RT modeling is inherently degenerate (Ivezic & Elitzur 1997) and hence models are not unique. Consequently, we use the modeling only to constrain  $\tau_{10\mu\text{m}}$  and to determine which minerals are inconsistent with the observed spectral features. A detailed analysis of the model results will be presented elsewhere.

At pressures relevant to I17495,  $T_{\text{dust}} \approx 1200$  K for  $\text{Mg}_2\text{SiO}_4$  and  $\text{MgSiO}_3$ . Models with  $T_{\text{dust}} < 800$  K could not match the observations because the near-IR becomes too bright, and in the mid-IR the spectrum slopes the wrong way. One important result of the modeling is that pyroxenes can be excluded from the mineralogy in I17495. The underlying amorphous silicate feature is unusually narrow and peaks closer to  $10\mu\text{m}$  rather than  $9.7\mu\text{m}$ , consistent with  $\text{Mg}_2\text{SiO}_4$  glass (Ossenkopf et al. 1992, and references therein). Models incorporating amorphous silicate of pyroxene composition (e.g. Jäger et al. 1994) or other more silica-rich compositions (e.g. Ossenkopf et al. 1992) are inconsistent with the observed spectrum, as the peak position of the feature gets too blue, and the FWHM gets too wide. Increasing the iron content in olivine has a similar effect on the peak position (Ossenkopf et al. 1992). Our models suggest that the crystalline component is also dominated by forsterite with enstatite and other crystalline compositions limited to less than a few percent of the dust mass. Therefore, both amorphous and crystalline dust is dominated by  $\text{Mg}_2\text{SiO}_4$ . This observed forsteritic mineralogy needs to be understood in terms of dust formation mechanisms.

### 4. Competing dust formation mechanisms

There are effectively three competing dust formation mechanisms for circumstellar environments: (i) thermodynamic equilibrium condensation (Lodders & Fegley 1999); (ii) formation of chaotic solids in a supersaturated gas followed by annealing (Stencel et al. 1990); (iii) formation of seed nuclei in a supersaturated gas, followed by mantle growth (Gail & Sedlmayr

1999). The latter should follow thermodynamic equilibrium as long as density is high enough for gas-grain reactions to occur.

Several observational studies support the thermodynamic condensation sequence (Dijkstra et al. 2005; Blommaert et al. 2007), which is consistent with both (i) and (iii). In mechanism (ii), chaotic grains form with the bulk composition of the gas, and then anneal if the temperature is high enough (Stencel et al. 1990). This mechanism predicts that at low C/O ratios, the dust grains would comprise a mixture of olivine, pyroxene and silica, rather than be dominated by olivine alone. At high C/O ratios, Al-O bonds are predicted to form preferentially, leading to dust dominated by oxides rather than silicates. These predictions are inconsistent with observations (Dijkstra et al. 2005; Blommaert et al. 2007).

In the seed-mantle model,  $\text{Mg}_2\text{SiO}_4$  is expected to use more refractory condensates as nucleation centers (e.g.  $\text{Al}_2\text{O}_3$ ; see Fig. 2). Whether the transformation into  $\text{MgSiO}_3$  by gas-grain reaction occurs is then dependent on gas density. Condensation and annealing experiments show that the resulting dust is dominated by forsterite; enstatite is present only in trace amounts (e.g. Day & Donn 1978; Nuth & Donn 1982; Hallenbeck et al. 1998). In laboratory experiments, the density is always high compared to circumstellar shells, so they may only be relevant to the highest  $\dot{M}$ .

The modeled mineralogy is consistent with an abrupt decrease in density between the formation temperatures for forsterite and enstatite. Once  $\sim 20\%$  of the Si atoms are incorporated into dust, the opacity is such that radiation pressure accelerates the circumstellar material, resulting in a precipitous density decrease, and inhibiting further gas-grain reactions (Gail & Sedlmayr 1999). At high  $\dot{M}$ , forsterite is stable at a higher temperature than enstatite. Formation of forsterite grains provides the impetus for radiation-driven acceleration and thus reduces the efficacy of enstatite formation, leaving gas that is depleted in Mg and thus more silica-rich. Without a surface on which to nucleate, silicates will tend to form amorphous solids rather than crystals (Tsukamoto et al. 2001), thus the seed nuclei are of the utmost importance to forming crystalline grains. Moreover, the dispersion due to radiation pressure may lead to seedless amorphous dust formation in the low density gas, which should be slightly more silica-rich than  $\text{MgSiO}_3$  due to the depletion of Mg into forsterite grains. The glass composition should tend towards  $\text{Mg}_2\text{Si}_3\text{O}_8$ , which is one of the metastable compositions predicted by Rietmeijer et al. (1999).

It is possible that the appearance of the clear crystalline absorption feature in I17495 is related not to increased crystallinity, but rather to less masking of the feature as a result of similar crystalline and amorphous silicate compositions (see Kemper et al. 2001). This still leaves the question of why this source is different – how can this source have both its crystalline and amorphous dust components dominated by  $\text{Mg}_2\text{SiO}_4$ , given that the bulk

composition of the gas is closer to  $\text{MgSiO}_3$ ?

## 5. Factors influencing crystallinity and mineralogy

The physical factors which could give rise to the extremely high crystal content include: (1)  $\dot{M}$ ; (2)  $v_{\text{exp}}$ ; (3) metallicity; (4) C/O ratio.  $\dot{M}$  for I17495 is high, but similar to OH/IR stars and other color mimics, suggesting that  $\dot{M}$  alone cannot explain the high degree of crystallinity exhibited by this source. A low  $v_{\text{exp}}$  would increase the pressure at a given temperature and thus promote grain formation/growth at higher temperatures. However,  $v_{\text{exp}}$  for I17495 is relatively high. Increasing metallicity increases the partial pressure of the dust forming elements, and thus increases the dust formation temperature at a given total gas pressure. The metallicity of the source is unknown, although its location in the Galactic plane suggests that it may have higher than solar metallicity. If metallicity were the determining cause, we would expect to see similar spectra in the GB OH/IR stars. The fact that even the high  $\dot{M}$  GB stars do not exhibit such a distinct crystalline silicate feature suggests that a combination of  $\dot{M}$  and metallicity would also fail to increase the crystal fraction.

Having eliminated  $\dot{M}$ ,  $v_{\text{exp}}$  and metallicity as likely causes of higher crystallinity, we are left with C/O ratio as the most likely culprit. The condensation scheme suggested in § 4 is relevant to solar C/O ( $\approx 0.48$ ). Oxygen-rich AGB stars have C/O ratios between 0.4 and 0.8, where the exact value depends on both the initial mass and age of the star; increasing this ratio decreases the availability of oxygen atoms with which to make dust.

The Mg/Si ratio in the circumstellar outflow from which the dust forms is close to unity. The silica-poor composition of the amorphous dust requires sequestration of some silicon into a non-silicate phase to increase the Mg/Si ratio (c.f. Ferrarotti & Gail 2001). While the formation of gehlenite ( $\text{Ca}_2\text{Al}_2\text{SiO}_7$ ) before the Mg-rich silicates is predicted in many condensation models (e.g Lodders & Fegley 1999; Gail & Sedlmayr 1999; Tielens 1990, and references therein), Si/Ca  $\sim 16$ , and thus gehlenite is not an effective sink for silicon atoms.

Other options would be keeping the Si in gas phase SiO; or condensation of Si into a metallic (or other featureless) phase (e.g. FeSi). The predicted path by which  $\text{MgSiO}_3$  forms is a reaction of  $\text{Mg}_2\text{SiO}_4$  with SiO gas, requiring an additional oxygen atom. Consequently, high C/O may limit the conversion of  $\text{Mg}_2\text{SiO}_4$  into  $\text{MgSiO}_3$  and preserve a silica-poor mineralogy. The condensation of FeSi is predicted for C/O ratios  $> 0.65$  (Ferrarotti & Gail 2002; Lodders & Fegley 1999). As C/O approaches unity,  $T_{\text{dust}}$  for the Mg-silicates decreases rapidly (Lodders & Fegley 1997) and Si is more apt to be incorporated into FeSi

(Ferrarotti & Gail 2002). For  $C/O > 0.85$ , the Mg-silicate dust formation temperature drops to below that of FeSi (Ferrarotti & Gail 2002), which results in sequestration of Si and increases the Mg/Si ratio of the gas from which the silicates form. Therefore, there are at least two mechanisms by which higher C/O ratios may be able to explain the composition of I17495.

Based on the preceding arguments we suggest that a high C/O ratio is the cause of the unusual mineralogy of I17495. Our hypothesis predicts several observable correlations: (1) between the strength of SiO absorption and C/O ratio in low  $\dot{M}$  stars; (2) between SiO absorption and the relative abundances of crystalline forsterite and enstatite in high  $\dot{M}$  stars; and (3) between C/O and the peak positions/FWHM of the classic  $10\mu\text{m}$  (emission) feature. As discussed in § 3 the peak position and FWHM of the  $10\mu\text{m}$  feature depend on the composition of the amorphous silicate.

## 6. The effect of source morphology

Molster et al. (1999, 2002) found a correlation between AGB/post-AGB star crystallinity and source morphology, with “disk-like” sources having a higher degree of crystallinity than spherical sources. Molster et al. (1999) suggested that this correlation is due to low-temperature crystallization in a long-lived disk. However, the inference of a disk around highly crystalline sources comes from imaging and the general shape of the SED, which cannot distinguish between a Keplerian disk and a toroidal outflow. There is evidence that the last stages of mass loss from AGB stars become increasing toroidal, and that this effect is stronger the more massive the progenitor star (Dijkstra & Speck 2006, and references therein). In this case, the density/pressure in the dust-forming regions would be enhanced further by the concentration of material into the star’s equatorial region, leading to conditions more apt to form crystalline structures. This in turn would correlate degree of crystallinity with initial mass of the star. Only massive AGB stars would produce significant amounts of crystalline material, and these are significantly rarer than low mass AGB stars. This resolves the conundrum of the ISM (having low crystallinity) being enriched by high crystallinity sources (see § 1).

## 7. Conclusions

We have presented the first crystalline silicate absorption feature observed to date. The spectrum of I17495 is enigmatic and suggests that its dust is dominated by  $\text{Mg}_2\text{SiO}_4$  in

both the crystalline and amorphous phases. We have confirmed that high mass-loss rates should produce more crystalline material than low mass-loss rates; and that the crystalline mineralogy should be increasingly dominated by forsterite as mass-loss rates increase. The most likely factor controlling both crystallinity and mineralogy is the C/O ratio. We suggest that the correlation between crystallinity, mass-loss rate and initial stellar mass mitigates the problem of the very different crystal fractions observed in some AGB stars and in the ISM. Only the rarer, higher mass AGB stars contribute a significant amount of crystalline material to the ISM.

We are grateful to H.-P. Gail, whose comments significantly improved this paper. This work is supported by NSF CAREER AST-0642991 (for A.K.S.) and NSF CAREER EAR-0748411 (for A.G.W.).

## REFERENCES

- Blommaert, J., et al., 2007, in *Why Galaxies Care About AGB Stars: Their Importance as Actors and Probes*, F. Kerschbaum, C. Charbonnel, and R. F. Wing, Eds. ASP Conference Series 378, Astronomical Society of the Pacific, San Francisco, pp.164.
- Boersma, C., 2008, *A&A*, 484, 241.
- Cami, J., de Jong, T., Justtanont, K., Yamamura, I., Waters, L. B. F. M., 1998, *Ap&SS*, 255, 339
- Crovisier, J. et al., 1996, *A&A*, 315, L385.
- Day, K.L., Donn, B. 1978, *ApJ*, 222, L45.
- Dijkstra, C., Speck, A. K., Reid, R. B., Abraham, P., 2005, *ApJ*, 633, L133.
- Dijkstra, C., Speck, A.K., 2006, *ApJ*, 651, 288 (2006).
- Gail, H.-P., Sedlmayr, E., 1999, *A&A*, 347, 594.
- de Graauw, T. et al., 1996, *A&A*, 315, 49.
- Fabian, D., et al., 2001, *A&A*, 378, 228.
- Ferrarotti, A. S., Gail, H.-P., 2002, *A&A*, 382, 256.
- Ferrarotti, A. S., Gail, H.-P., 2001, *A&A*, 371, 133.

- Hallenbeck, S. L., Nuth, J. A., III, Daukantas, P. L., *Icarus*, 131, 198.
- Ivezic, Z., Elitzur, M., 1995, *ApJ*, 445, 415.
- Ivezic, Z., Elitzur, M., 1997, *MNRAS*, 287, 799.
- Jäger, C., Mutschke, H., Begemann, B., Dorschner, J., Henning, Th., 1994, *A&A*, 292, 641.
- Jäger, C., et al. 1998, *A&A*, 339, 904.
- Kemper, F., et al., 2004, *ApJ*, 609, 806.
- Kemper, F., Waters, L. B. F. M., de Koter, A., Tielens, A. G. G. M., 2001, *A&A*, 369, 132.
- Koike, C., et al., 2003, *A&A*, 399, 1101.
- Kwok, S., 2004, *Nature*, 430, 985.
- Lewis, B.M., 1994, *A&A*, 288, L5.
- Lodders, K. Fegley, B., Jr., 1997, *AIP Conf. Proc.* 402, *Astrophysical Implications of the Laboratory Study of Presolar Materials*, ed. T. J. Bernatowicz & E. Zinner (New York: AIP), 391.
- Lodders, K. Fegley, B., Jr., 1999, in *Asymptotic Giant Branch Stars, IAU Symposium 191*, T. Le Bertre, A. Lebre, and C. Waelkens, Eds., p279.
- Loup, C., Forveille, T., Omont, A., Paul, J. F., 1993, *A&AS*, 99, 291.
- Min, M., et al., 2007, *A&A*, 462, 667.
- Molster, F.J., et al., 1999, *Nature*, 401, 563.
- Molster, F. J., Waters, L. B. F. M., Tielens, A. G. G. M., 2002, *A&A*, 382, 222.
- Nuth, J. A., III, Donn, B., 1982, *ApJ*, 257, L103.
- Ossenkopf, V., Henning, Th., Mathis, J. S., 1992, *A&A*, 261, 567.
- Richet, P., Leclerc, F., Benoist, L., 1993, *Geophys. Res. Lett.*, 20, 1675.
- Rietmeijer, F.J.M., Nuth, J. A., III, Karner, J.M., 1999, *ApJ*, 527, 395.
- Sogawa, H., Kozasa, T., 1999, *ApJ*, 516 L33.
- Speck, A. K., Barlow, M. J., Sylvester, R. J., Hofmeister, A. M., 2000, *A&AS*, 146, 437.

- Spoon, H. W. W., et al., 2006, ApJ, 638, 759.
- Stencel, R. E., Nuth, J. A., III, Little-Marenin, I. R., Little, S. J., 1990, ApJ, 350, L45.
- Sylvester, R.J., et al., 1999, A&A, 352, 587.
- Tamanai, A., Mutschke, H., Blum, J., Meeus, G., 2006, ApJ, 648, L147.
- Tielens, A.G.G.M., 1990, in: From Miras to planetary nebulae: Which path for stellar evolution?; Proceedings of the International Colloquium, (A91-46697 20-90). Gif-sur-Yvette, France, Editions Frontieres, 1990, p. 186.
- Tsukamoto, K., Kobatake, H., Nagashima, K., Satoh, H., Yurimoto, H., 2001, Lunar Planet. Sci. Conf., XXXII, abstract # 1846 .
- Vanhollebeke, E., 2007, Ph.D. thesis, KU Leuven, Belgium.
- van Loon, J. T., Cioni, M.-R. L., Zijlstra, A.A., Loup, C., 2005, A&A, 438, 273.
- Waelkens, C. et al., 1996, A&A, 315, L245.
- Waters, L. B. F. M., et al., 1996, A&A, 315, L361.
- Wilding, M. C., Benmore, C. J., Tangeman, J. A., Sampath, S., 2004, Europhys. Lett., 67, 212.

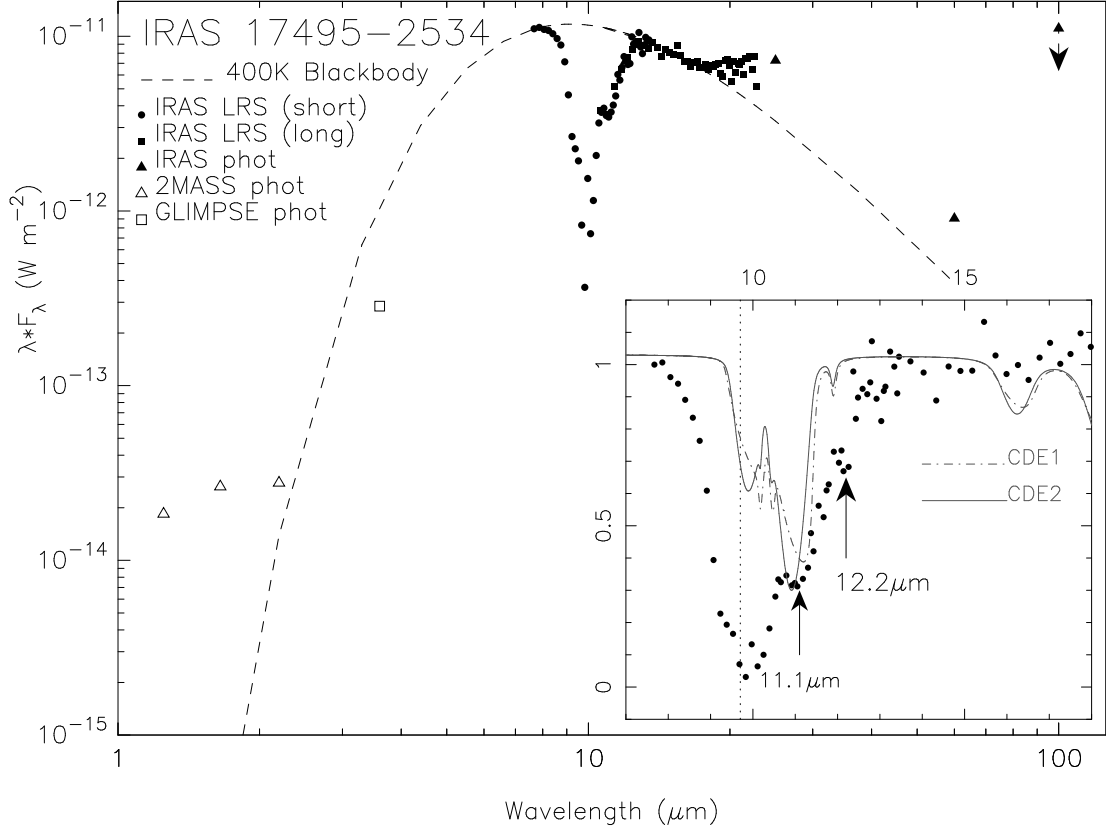


Fig. 1.— The spectrum of IRAS 17495–2534:  $y$ -axis is flux ( $\lambda F_\lambda$ ) in  $\text{W m}^{-2}$ . *Main panel:* log-log plot of the full spectral energy distribution (SED) including the IRAS LRS spectrum, the near-IR JHK photometry from 2MASS,  $3.6\mu\text{m}$  photometry from the Spitzer GLIMPSE survey, and far-IR photometry points from IRAS. *Inset:* linear-scale close-up on the continuum-divided IRAS LRS spectrum, with crystalline features indicated by arrows.  $y$ -axis is normalized flux. Grey lines are calculated mass absorption coefficients for continuous distributions of ellipsoidal (CDE) crystalline forsterite grains from Fabian et al. (2001). CDE1 has equal probability of all shapes; CDE2 has quadratic weighting, such that near-spherical particles are most probable. Dotted line at  $9.7\mu\text{m}$  is included to demonstrate the redness of the peak of the absorption feature.

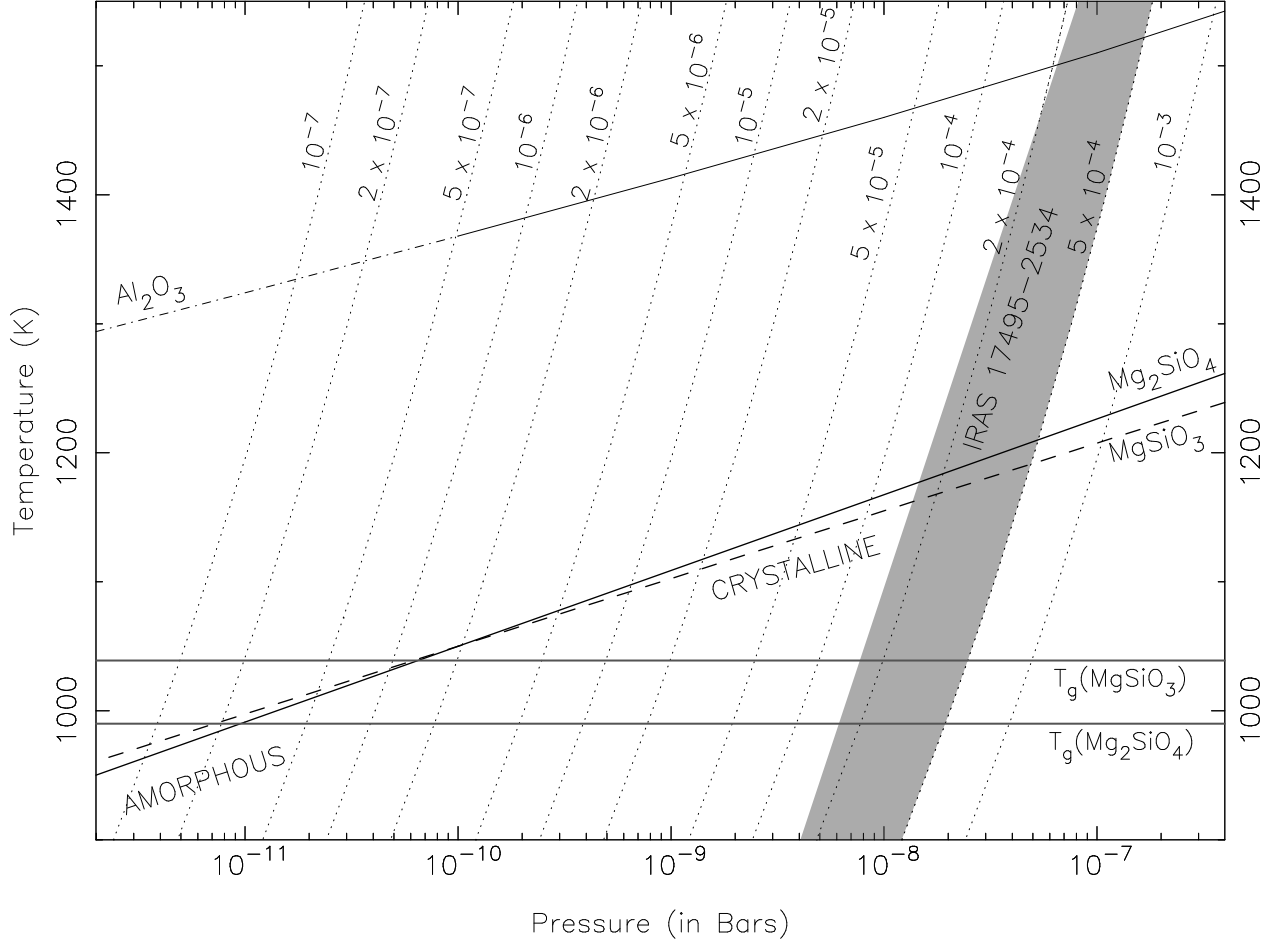


Fig. 2.— P–T space for dust condensation around O-rich AGB stars: Solid and dashed lines indicate  $T_{\text{dust}}$  for a given pressure from thermodynamic equilibrium calculations (relevant compositions are labeled) (Lodders & Fegley 1999). The stability temperature of  $\text{Al}_2\text{O}_3$  is dot-dashed where extrapolated. For all  $\dot{M}$  values,  $\text{Al}_2\text{O}_3$  forms at a significantly higher temperature than the silicates, and thus can form a seed nucleus. Dotted lines indicate the P–T paths for the outflowing gas for a range of  $\dot{M}$  (indicated in  $M_{\odot}/\text{yr}$ ) as calculated from  $\dot{M}$  and  $v_{\text{exp}}$ . Thick grey horizontal lines indicate  $T_g$  for  $\text{Mg}_2\text{SiO}_4$  and  $\text{MgSiO}_3$ . Grey shaded area shows the P–T space relevant to I17495.